2D higher-order theories for progressive damage model of composite structures based on Hashin and Puck failure criteria

Materials Research Proceedings 42 (2024) 61-65 https://doi.org/10.21741/9781644903193-14

2D higher-order theories for progressive damage model of composite structures based on Hashin and Puck failure criteria

Elisa Tortorelli[1,a *], Salvatore Saputo[1,b] and Erasmo Carrera[1,c]

[1]Department of Mechanical and Aerospace Engineering, Politecnico di Torino, Turin, Italy, 10129

[a]elisa.tortorelli@polito.it, [b]salvatore.saputo@polito.it, [c]erasmo.carrera@polito.it

Keywords: CUF, Explicit Damage Modelling, Failure Criteria

Abstract. This paper proposes a high-order 2D finite element model for the progressive damage model of composite structures. The model is based on Carrera Unified Formulation (CUF), which allows to automatically implement different kinematics by using an opportune recursive notation. A Newton-Raphson algorithm and the explicit integration scheme is used to find the converged solution. A single element and an open-hole specimen under tensile and compression loads are investigated using a damage model based on Hashin and Puck failure criteria. The proposed model is compared with literature and ABAQUS continuum shell results.

Introduction

In recent decades, advanced fiber-reinforced composites have significantly integrated into various high-performance applications, including the aerospace, automotive, and maritime sectors. Nevertheless, composite materials are not immune from degradation, damage and nonlinear behavior. There are numerical tools for modeling progressive failure of composite across scales through development of computationally-efficient advanced structural models, as micromechanical progressive failure analysis [1].

Computational damage models for composite structures can be broadly categorized into two main approaches. The first approach, known as discrete modeling, entails the explicit geometrical representation of cracks within the structure, but it comes with significantly heightened computational demands. A different approach to discrete damage modeling involves continuum damage mechanics (CDM), which preserves the continuity of the displacement field within the finite element mesh [2] showing low computational cost. The fracture energy is used to mitigate a strong mesh dependency. A purely continuum damage approach is described in Ref. [3], focusing on intralaminar damage within the ply, which is characterized using the Composite Damage (CODAM) model. In particular, it is used the second-generation damage model, CODAM2 which is a strain-based damage formulation [4].

This paper consider a new damage model based on Hashin 3D failure criteria and Puck's failure criteria for matrix compression [6]. The model is compared with CODAM2 implemented by Nagaraj et al. [5], which is based on Hashin 2D failure criteria. The structural modelling is built in the framework of the Carrera Unified Formulation (CUF) [7] which allows employing higher-order structural theories to develop refined 1D and 2D models where the kinematic field is enriched via the use of cross-section and thickness expansion functions, respectively. This approach reduces the computation cost compared with standard solid elements FE analyses. The explicit integration scheme is used to find the converged solution.

Failure criteria and damage model

The CODAM2 material model implemented in the CUF framework has been previously explained in Ref. [5, 8], which consider Hashin 2D quadratic failure criterion for fiber and matrix tensile/compression. In this paper, instead, three-dimensional Hashin criteria are implemented for

Materials Research Proceedings 42 (2024) 61-65 https://doi.org/10.21741/9781644903193-14

matrix, fiber tensile and fiber compression. For matrix compression Puck criterion was considered. In Fig. 1, failure criteria implemented in this paper are shown

HASHIN 3D / PUCK	TENSILE	COMPRESSION
FIBER	$F_{ft} = \left(\frac{\sigma_{11}}{X_t}\right)^2 + \alpha_f \left[\left(\frac{\sigma_{12}}{S_{12}}\right)^2 + \left(\frac{\sigma_{13}}{S_{13}}\right)^2\right] \geq 1$	$F_{fc} = \left(\frac{\sigma_{11}}{X_c}\right)^2 \geq 1$
MATRIX	$F_{mt} = \left(\frac{\sigma_{22}+\sigma_{33}}{Y_t}\right)^2 + \frac{1}{S_{23}^2}(\sigma_{23}^2 + \sigma_{22}\sigma_{33}) + \left(\frac{\sigma_{12}}{S_{12}}\right)^2 + \left(\frac{\sigma_{13}}{S_{13}}\right)^2 \geq 1$	$F_{mc} = \left(\frac{\sigma_{nt}}{S_{23}^A - \eta_{nt}\sigma_{nn}}\right)^2 + \left(\frac{\sigma_{nl}}{S_{12} - \eta_{nl}\sigma_{nn}}\right)^2 \geq 1$

Figure 1. Hashin 3D failure criteria for tensile/compression fiber and tensile matrix. Puck failure criterion for compression matrix.

where $X_T,\ X_c,\ Y_T, Y_c$ are the fiber and matrix tensile/compression, respectively; all parameters in Puck's criterion ca be found in [9]. The equivalent strain measures for tensile/compression in the longitudinal and transverse directions are defined as

$$\delta_{eq}^{ft} = l_c\sqrt{\langle\varepsilon_{11}\rangle^2 + \varepsilon_{12}^2 + \varepsilon_{13}^2}, \qquad \delta_{eq}^{mt} = l_c\sqrt{\langle\varepsilon_{22}\rangle^2 + \langle\varepsilon_{33}\rangle^2 + \varepsilon_{12}^2 + \varepsilon_{23}^2 + \varepsilon_{13}^2} \tag{1}$$

$$\delta_{eq}^{fc} = l_c\langle-\varepsilon_{11}\rangle, \qquad \delta_{eq}^{mc} = l_c\sqrt{\langle-\varepsilon_{22}\rangle^2 + \langle-\varepsilon_{33}\rangle^2 + \varepsilon_{12}^2 + \varepsilon_{23}^2 + \varepsilon_{13}^2} \tag{2}$$

The corresponding equivalent stress measures are given by

$$\sigma_{eq}^{ft} = \frac{l_c(\langle\sigma_{11}\rangle\langle\varepsilon_{11}\rangle + \sigma_{12}\varepsilon_{12} + \sigma_{13}\varepsilon_{13})}{\delta_{eq}^{ft}}, \quad \sigma_{eq}^{mt} = \frac{l_c(\langle\sigma_{22}\rangle\langle\varepsilon_{22}\rangle + \langle\sigma_{33}\rangle\langle\varepsilon_{33}\rangle + \sigma_{12}\varepsilon_{12} + \sigma_{23}\varepsilon_{23} + \sigma_{13}\varepsilon_{13})}{\delta_{eq}^{mt}} \tag{3}$$

$$\sigma_{eq}^{fc} = \frac{l_c\langle-\sigma_{11}\rangle\langle-\varepsilon_{11}\rangle}{\delta_{eq}^{fc}}, \qquad \sigma_{eq}^{mc} = \frac{l_c(\langle-\sigma_{22}\rangle\langle-\varepsilon_{22}\rangle + \langle-\sigma_{33}\rangle\langle-\varepsilon_{33}\rangle + \sigma_{12}\varepsilon_{12} + \sigma_{23}\varepsilon_{23} + \sigma_{13}\varepsilon_{13})}{\delta_{eq}^{mc}} \tag{4}$$

The damage d in the post-peak branch is defined as

$$d = \frac{\delta_{eq}^u(\delta_{eq} - \delta_{eq}^0)}{\delta_{eq}(\delta_{eq}^u - \delta_{eq}^0)} \tag{5}$$

where $\delta_{eq} = l_c\varepsilon_{eq}$ is the equivalent displacement and $\delta_{eq}^u = \frac{2G_\alpha}{\sigma_{eq}}$ is the equivalent displacement when the damage d=1; l_c is the characteristic length and it corresponds to the cubic root of Gauss point volume. It is possible to compute the secant stiffness matrix in the damaged state as

$$C_d = \frac{1}{\Delta}\begin{bmatrix} C_{11} & C_{12} & C_{13} & 0 & 0 & 0 \\ C_{21} & C_{22} & C_{23} & 0 & 0 & 0 \\ C_{31} & C_{32} & C_{33} & 0 & 0 & 0 \\ 0 & 0 & 0 & C_{44} & 0 & 0 \\ 0 & 0 & 0 & 0 & C_{55} & 0 \\ 0 & 0 & 0 & 0 & 0 & C_{66} \end{bmatrix} \tag{6}$$

More detailed description of secant stiffness matrix in the damage state can be found in [8].

Materials Research Proceedings 42 (2024) 61-65 https://doi.org/10.21741/9781644903193-14

2D Carrera Unified formulation

CUF allows writing the equations of any refined theory 1D, 2D, or 3D in terms of a few fundamental nuclei FNs. The three-dimensional displacement field $\boldsymbol{u}(x,y,z)$ can be expressed as a product between a 2D in-plane shape function $N_i(x,y)$ of order p and 1D expansion function $F_\tau(z)$:

$$\boldsymbol{u}(x,y,z) = N_i(x,y)F_\tau(z)\boldsymbol{u}_{\tau i} \qquad \tau = 1,\dots,M \qquad i = 1,\dots,p+1 \tag{7}$$

More detailed of 2D plate modelling in CUF can be found in Ref. [10]. The linear strain-displacement relation is then expressed as $\boldsymbol{\varepsilon} = \boldsymbol{B}\boldsymbol{u}$, where $\boldsymbol{B}$ is the differential operator. The constitutive relation is given by $\boldsymbol{\sigma} = \boldsymbol{C}^{sec}$, where $\boldsymbol{C}^{sec}$ is obtained from damage model described in the previous section.

Numerical results

In this section, two cases of numerical assessments are shown. The material system used is IM7/8552 carbon fiber reinforced polymer (CFRP) with ply thickness of 0.125 mm, Table 1.

Table 1. Material properties of the IM7/8552 carbon fiber reinforced polymer.

E_1 [GPa]	E_2 [GPa]	E_3 [GPa]	G_{12} [GPa]	G_{13} [GPa]	G_{23} [GPa]	ν_{12}	ν_{13}	ν_{23}
150.0	11.0	11.0	5.8	5.8	2.9	0.34	0.34	0.48
X_T [MP]	X_C [MP]	Y_T [MPa]	Y_C [MPa]	S_{12} [MPa]	G_1^T [kJ/m^2]	G_2^T [kJ/m^2]	G_1^C [kJ/m^2]	G_2^C [kJ/m^2]
2560.0	1690.0	73.0	250.0	90.0	120.0	2.6	80.0	4.2

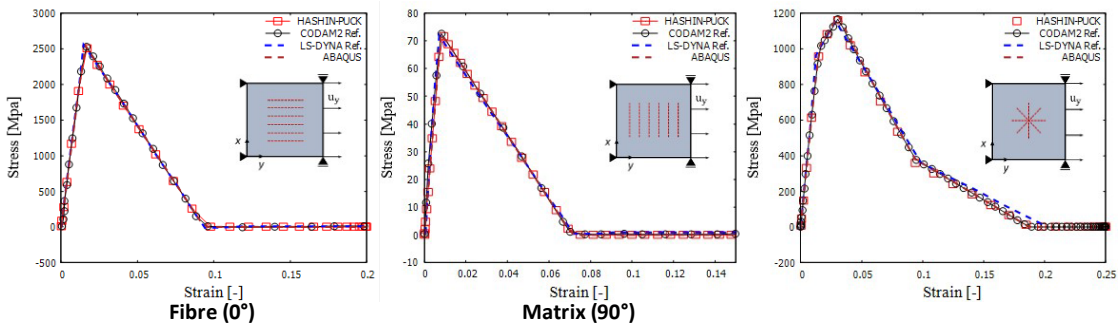

Figure 2. Stress-strain response of the single element under tensile loading with fiber orientation of 0°, 90° and [90/45/0/-45]$_{2s}$, respectively. Comparison with ABAQUS response, CODAM2 Ref. [5] and LS-DYNA Ref. [11].

The first case refers to a single of size $1\,mm \times 1\,mm$ with under uni-axial strain conditions both for tensile and compression loading. Three tests are considered referring to loading in the longitudinal direction (along the fiber 0°), in the transverse direction (perpendicular to the fiber 90°) and considering a quasi-isotropic [90/45/0/-45]$_{2s}$ laminate. The in-plane discretization consists of one Q4 element and each ply thickness is modeled via a single linear (LE1) Lagrange polynomial. In Fig. 2, the stress-strain response of the single element under tensile loading with fiber orientation of 0°, 90° and [90/45/0/-45]$_{2s}$ laminate, respectively. The response is obtained by Hashin-Puck damage model correlates well with numerical reference CODAM2 [5], LS-DYNA [11] and ABAQUS model. Similarly, the stress-strain response of the single element under compressive loading is shown in Fig. 3, compared to ABAQUS, CODAM2 [8] and LS-DYNA [11] response.

Materials Research Proceedings 42 (2024) 61-65 https://doi.org/10.21741/9781644903193-14

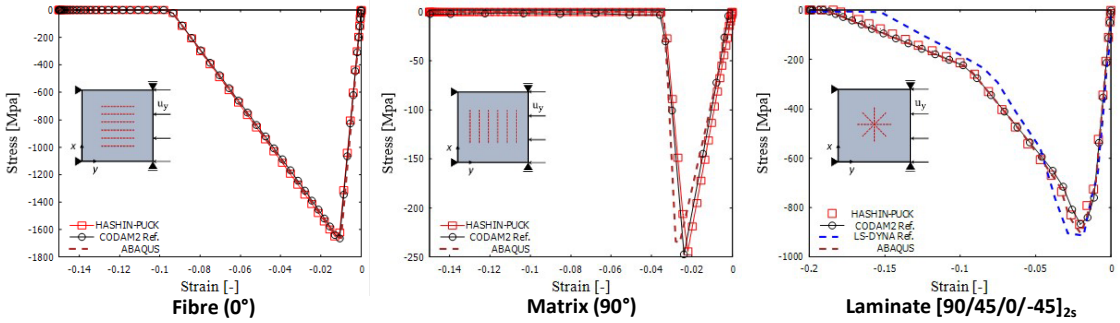

Figure 3. Stress-strain response of the single element under compression loading with fiber orientation of 0°, 90° and $[90/45/0/-45]_{2s}$, respectively. Comparison with ABAQUS response, CODAM2 Ref. and LS-DYNA Ref [5].

The next numerical assessment refers to an open-hole $[45/90/-45/0]_{2s}$ laminates of size $32\,mm \times 32\,mm$ subjected to compressive loads. In Fig. 4, the predictive failure strength computed with Hashin-Puck damage model and compared with ABAQUS, CODAM2 [8] and experiment [12] results.

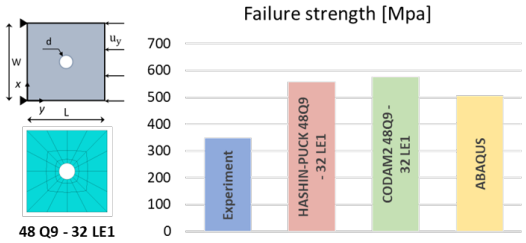

Figure 4. Comparison of failure strength of the open-hole $[45/90/-45/0]_{2s}$ specimen compared with experiment [12], CODAM2 [8] and ABAQUS results.

Conclusions

The current work presents the development of damage model based on Hashin 3D failure criteria and Puck's failure criteria for matrix compression using higher-order structural theories based on CUF. Three assessments are shown refers to a single elements, under tensile and compressive loading, and an open-hole specimen under compressive loading. The predictions of the proposed framework were in good general agreement with reference numerical and experimental results. The validation of this damage model highlights the advantages of CUF in computational costs. Future investigations include extending the present work to more complex structural problems. Other future works include modeling progressive failure of composite across scales through development of computationally-efficient advanced structural models, as micromechanical progressive failure analysis.

References

[1] I. Kaleel, M. Petrolo and E. Carrera, Elastoplastic and progressive failure analysis of fiber-reinforced composites via an efficient nonlinear microscale model, Aerotecnica Missili & Spazio, vol. 97, pp. 103-110, 2018.

[2] P. Ladeveze and E. LeDantec, Damage modelling of the elementary ply for laminated composites, Composites Science and Technology, vol. 43, no. 3, pp. 257-267, 1992. https://doi.org/10.1016/0266-3538(92)90097-M

[3] K. V. Williams, R. Vaziri and A. Poursartip, A physically based continuum damage mechanics model for thin laminated composite structures, International Journal of Solids

and Structures, vol. 40, no. 9, pp. 2267-2300, 2003. https://doi.org/10.1016/S0020-7683(03)00016-7

[4] A. Forghani, N. Zobeiry, A. Poursartip and R. Vaziri, A structural modelling framework for prediction of damage development and failure of composite laminates, Journal of Composite Materials, vol. 47, no. 20, pp. 2553-2573, 2013. https://doi.org/10.1177/0021998312474044

[5] M. H. Nagaraj, J. Reiner, R. Vaziri, E. Carrera and M. Petrolo, Progressive damage analysis of composite structures using higher-order layer-wise elements, Composites Part B: Engineering, vol. 190, 2020. https://doi.org/10.1016/j.compositesb.2020.107921

[6] L. Bek, R. Kottner and V. Laš, Material model for simulation of progressive damage of composite materials using 3D Puck failure criterion, Composite Structures, vol. 259, 2021. https://doi.org/10.1016/j.compstruct.2020.113435

[7] E. Carrera, M. Cinefra, M. Petrolo and E. Zappino, Finite element analysis of structures through unified formulation, John Wiley & Sons, 2014.

[8] M. H. Nagaraj, J. Reiner, R. Vaziri, E. Carrera and M. Petrolo, Compressive damage modeling of fiber-reinforced composite laminates using 2D higher-order layer-wise models, Composites Part B: Engineering, vol. 215, 2021. https://doi.org/10.1016/j.compositesb.2021.108753

[9] X. Li, D. Ma, H. Liu, W. Tan, X. Gong, C. Zhang and Y. Li, Assessment of failure criteria and damage evolution methods for composite laminates under low-velocity impact, Composite structures, vol. 207, pp. 727-739, 2019. https://doi.org/10.1016/j.compstruct.2018.09.093

[10] E. Zappino, G. Li, A. Pagani and E. Carrera, Global-local analysis of laminated plates by node-dependent kinematic finite elements with variable ESL/LW capabilities, Composite Structures,, vol. 172, pp. 1-14. https://doi.org/10.1016/j.compstruct.2017.03.057

[11] J. Reiner, T. Feser, D. Schueler, M. Waimer and R. Vaziri, Comparison of two progressive damage models for studying the notched behavior of composite laminates under tension, Composite Structures, vol. 207, pp. 385-396, 2019. https://doi.org/10.1016/j.compstruct.2018.09.033

[12] J. Lee and C. Soutis, Measuring the notched compressive strength of composite laminates: Specimen size effects, Composites Science and Technology, vol. 68, no. 12, pp. 2359-2366, 2008. https://doi.org/10.1016/j.compscitech.2007.09.003